Biomaterials 32 (2011) 5471–5477

Contents lists available at ScienceDirect

Biomaterials

journal homepage: www.elsevier.com/locate/biomaterials

One-to-one quantum dot-labeled single long DNA probes

Shibin He [a,1], Bi-Hai Huang [b,1], Junjun Tan [a], Qing-Ying Luo [b], Yi Lin [b], Jun Li [a], Yong Hu [a], Lu Zhang [a], Shihan Yan [a], Qi Zhang [a], Dai-Wen Pang [b,*], Lijia Li [a,**]

[a] State Key Laboratory of Hybrid Rice, College of Life Sciences, Wuhan University, Wuhan 430072, PR China
[b] Key Laboratory of Analytical Chemistry for Biology and Medicine (Ministry of Education), College of Chemistry and Molecular Sciences, Research Center for Nanobiology and Nanomedicine (MOE 985 Innovative Platform), and State Key Laboratory of Virology, Wuhan University, Wuhan 430072, PR China

ARTICLE INFO

Article history:
Received 18 March 2011
Accepted 5 April 2011
Available online 5 May 2011

Keywords:
Nanoparticle
DNA
PCR (polymerase chain reaction)
In situ hybridization

ABSTRACT

Quantum dots (QDs) have been received most attention due to their unique properties. Constructing QDs conjugated with certain number of biomolecules is considered as one of the most important research goals in nanobiotechnology. In this study, we report polymerase chain reaction (PCR) amplification of primer oligonucleotides bound to QDs, termed as QD-based PCR. Characterization of QD-based PCR products by gel electrophoresis and atomic force microscopy showed that QD-labeled long DNA strands were synthesized and only a single long DNA strand was conjugated with a QD. The QD-based PCR products still kept fluorescence properties. Moreover, the one-to-one QD-labeled long DNA conjugates as probes could detect a single-copy gene on maize chromosomes by fluorescence *in situ* hybridization. Labeling a single QD to a single long DNA will make detection of small single-copy DNA fragments, quantitative detection and single molecule imaging come true by nanotechnology, and it will promote medical diagnosis and basic biological research as well as nano-material fabrication.

1. Introduction

Nanoparticle/biomolecule conjugates have been widely applied in biological sciences and material sciences due to their fascinating chemical and physical properties [1–5]. Among many biomolecules, DNA is well suited to construct functional nanomaterials for various applications because of its natural molecular recognition and structure properties [6]. In current research, one of the main challenges is how to precisely control the number of DNA strands conjugated to each nanoparticle, especially for a single nanoparticle labeling a single DNA strand that is very essential for quantitative analysis and single molecule imaging [7,8]. Many efforts have been made to prepare the nanoparticle conjugated with certain number of DNA strands, among which the most commonly used method is gel electrophoresis [9,10]. However, it is difficult to separate the nanoparticle with certain number of short DNA strands from a mixture by gel electrophoresis, and only oligonucleotides (<100 bases) can be efficiently conjugated to nanoparticles by the routine chemistry method due to steric hindrance and electrostatic repulsion [7,9].

Polymerase chain reaction (PCR) that can synthesize long DNA strands and exponentially amplify target DNA or RNA to generate a large number of DNA copies in a short period of time is one of the most popular and powerful methods in modern life sciences [11]. DNA bound to a variety of planar surfaces, including glass, magnetic bead [12] and, recently, Au nanoparticle has been used in PCR amplification [13] as well as in the extension [14] and restriction endonuclease reactions [15]. Core/shell CdSe/ZnS quantum dot (QD) -bound DNA has been enzymatically telomerized and replicated in vitro [16]. However enzymatic amplification of DNA bound to QDs presents some challenges not met in nylon or glasses based DNA enzymic analysis. For example, these semiconductor nanocrystal-bound oligonucleotides may suffer from steric hinderance during hybridization and enzymatic extension [14]; after PCR of a short oligonucleotide bound to a QD particle, it is unclear if a longer DNA fragment is still conjugated to the particle. QDs were significantly brighter and more photostable during excitation than organic fluorophores, which enables QDs as an ideal label [17–19]. The successful PCR amplification of DNA sequences conjugated to QDs would allow sensitive cell imaging as well as material fabrication [6,20].

In this study, we proposed a modified PCR strategy (called QD-based PCR) to construct single QD-labeled single long DNA strands by an enzymatic extension of the short primers covalently bound to the surface of relatively small QDs. Analysis using gel

* Corresponding author. Tel./fax: +86 27 68754067.
** Corresponding author. Tel./fax: +86 27 68754505.
E-mail addresses: dwpang@whu.edu.cn (D.-W. Pang), ljli@whu.edu.cn (L. Li).
[1] These authors contributed equally to this work.

0142-9612/$ – see front matter © 2011 Elsevier Ltd. All rights reserved.
doi:10.1016/j.biomaterials.2011.04.013

electrophoresis, atomic force microscopy (AFM) and fluorescence spectroscopy showed that a synthesized long DNA strand was coupled to a QD after PCR amplification and the QD conjugated with DNA still kept fluorescence properties. The one-to-one QD-labeled long DNA strands were explored to detect a single-copy gene on metaphase chromosomes, which still represents a great challenge in the traditional fluorescence *in situ* hybridization (FISH) [21]. Successful amplification of a single long DNA conjugated with a single QD is critical to sequence-specific DNA detection reported here, and it will promote medical diagnosis and basic biological research as well as nano-material fabrication.

2. Materials and methods

2.1. Synthesis of water soluble OPA-coated QDs

The core/shell CdSe/ZnS quantum dots were synthesized as described by ref. [22]. Before water solubilization, hexane-dispersed QDs were washed with methanol and resuspended in chloroform. Octylamine-modified polyacrylic acid (OPA) was synthesized based on a previous report [23]. Poly (acrylic acid) (PAA, 433 mg) and 1-ethyl-3-(3-dimethylaminopropyl) carbodiimide hydrochloride (EDC, 600 mg) were dissolved by N, N′-dimethylformamide (DMF), and octylamine (300 μl) was added to the solution. Then the mixture solution was stirred overnight, which could be monitored by a ninhydrin assay. When the reaction was completed, the product was washed with ultrapure water for several times and redissolved in methanol. After removing the solvent by a rotary evaporator, the yellow solid (OPA) was collected. Subsequently, excess OPA was added to CdSe/ZnS QDs (2 nmol) dissolved in chloroform. The solution was stirred for several minutes, and the solvent was removed by a rotary evaporator. The precipitate was redissolved in NaOH solution (pH = 9) and purified by size exclusion chromatography. The concentration of OPA-coated QDs was determined by UV-2550 spectrophotometer. Transmission electron microscope and dynamic light scattering measurement were used to analyze the QD size.

2.2. Preparation of QD-oligonucleotide conjugates

Oligonucleotide primers for a 480-bp sequence fragment of *fatty aldehyde dehydrogenase 1* in maize (GenBank database accession no. AY374447) were designed by Premier Primer 5.0 software. The forward primer sequence (P1) was 5′-NH_2-$(CH2)_6$-TTTTTT-GGCCTTCAGAGACGAGGTTG-3′ and the reverse primer sequence (P2) was 5′-GCTGTGCATCAGGAATAATTTG-3′. The 5′ amine-modified oligonucleotide primers (P1) were covalently coupled to the OPA-coated QDs surface in the presence of EDC and N-hydroxysuccinimide (NHS) as described previously with slight modification [24]. To minimize the potential steric hindrance, the primers (P1) contained a linker of homopolymer of thymine sequences and a C6 carbon chain to keep away from the QD [25]. The excess DNA was removed by repeated ultrafiltration (50 kDa, MWCO) until the subnatant did not contain DNA monitored by UV–Vis spectrometry and agarose gel electrophoresis. The final QD-oligonucleotide conjugates were dissolved in ultrapure water and stored at 4 °C.

2.3. PCR

Zea mays L. inbred line Huangzao 4 was used for the current research. Seeds were kindly provided by Professor Song Jiancheng (Shandong Agriculture University, Shandong Province, China). Genomic DNA was extracted from young maize leaves by using a cetyltriethylammnonium bromide (CTAB) method [26]. A 480 bp DNA fragment was obtained by amplification of genomic DNA using normal primers and cloned into Promega pGEM-T vector. Subsequently, PCR was performed with QD-P1 oligonucleotide conjugates and P2 primers using the cloned plasmid DNA as a template to minimize possible steric hindrance during amplification. PCR reactions were carried out at 94 °C for 4 min, followed by 35 cycles at 94 °C for 30 s, 60 °C for 30 s, and 72 °C for 1 min, with a final extension at 72 °C for 10 min. The QD-based PCR products were sequenced to confirm their identity. Sequencing was performed by Sangon Biochemistry Company (Shanghai, China).

2.4. Characterization of OPA-coated QDs, QD-oligonucleotide conjugates and QD-based PCR products

2.4.1. Transmission electron microscopy (TEM) imaging

Samples were prepared by placing a drop of the QD solution on a Formvar/carbon-coated copper grid and allowing the solvent to evaporate. The polymer coating was negatively stained by phosphotungstic acid. The TEM image was recorded with a H-7000 electron microscope (Hitachi, Tokyo, Japan).

2.4.2. Hydrodynamic diameter measurements by dynamic light scattering (DLS)

The DLS experiments were performed on the Nano ZS instrument (Malvern Instruments, Malvern, UK). All samples measured in this study were diluted by ultrapure water to the concentration of approximately 10-7 mol/L and transferred to a special dust free light scattering cell for measurement. The temperature of common measurements was controlled at 25 ± 0.02 °C. In the case of detecting the effect of the temperature on the size of QDs, the measurement was taken at a typical heating-cooling cycle (25 °C–85 °C).

2.4.3. UV–Visible and fluorescence measurements

Absorption spectra were acquired on a UV-2550 spectrophotometer (Shimadzu, Kyoto, Japan) and fluorescence spectra were recorded by a NanoLog spectrofluorometer (HORIBA Jobin Yvon, NJ, USA) using quartz cuvettes. Usually, measurements of both absorption and fluorescence spectra were performed at a room temperature using quartz cuvettes. In the case of estimating the effect of the temperature on fluorescence intensity of OPA coated-QDs, the temperature was controlled by a thermoelectric temperature controller (LFI-3751, Wavelength Electronics, MT, USA).

2.4.4. Gel electrophoresis

Mobility shift assay and Luminescence assay were done by gel electrophoresis to analyze the mobility shift of samples and QD luminescence. Five microliters of each sample were loaded in 1% agarose gel in Tris-Borate-EDTA buffer (TBE) and run at 120 V for 60 min. Digital image of the gel was captured with the AlphaImager IS-2200 (Alpha Innotech, CA, USA). And the gel was poststained with ethidium bromide (EB) to identify the DNA.

2.4.5. AFM imaging

AFM imaging was conducted with a PicoScan atomic force microscope (Molecular Imaging, CA, USA). Freshly prepared samples were mounted on AFM stage and imaged under MAC Mode in air (relative humidity = 40%–50%, T = ~25 °C) using MAClever type II probes (spring constant = 2.8 N/m, resonant frequency = ~85 kHz, Molecular Imaging, CA, USA). Scan rates were about 1.5 line/s. The images were rastered at 256 × 256 pixels, unfiltered and flattened when needed.

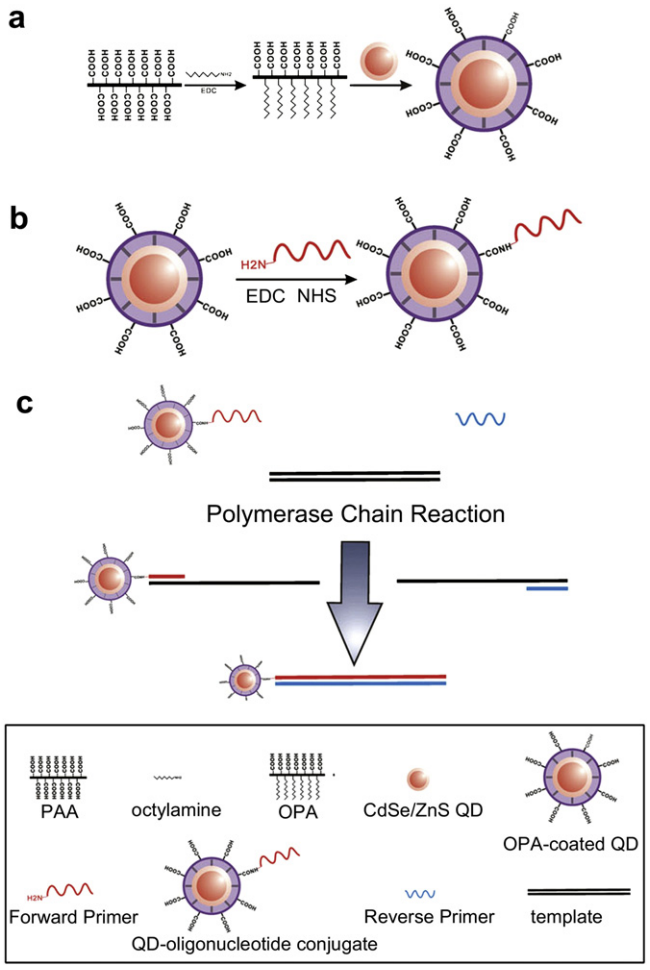

Fig. 1. Strategy for construction of the one-to-one QD-labeled single long DNA probes. (a) Synthesis of water soluble OPA-coated QDs. (b) Conjugation of the 5′ amine-modified primers to the surface of OPA-coated QDs. (c) Extension of the QD-oligonucleotide conjugates by PCR.

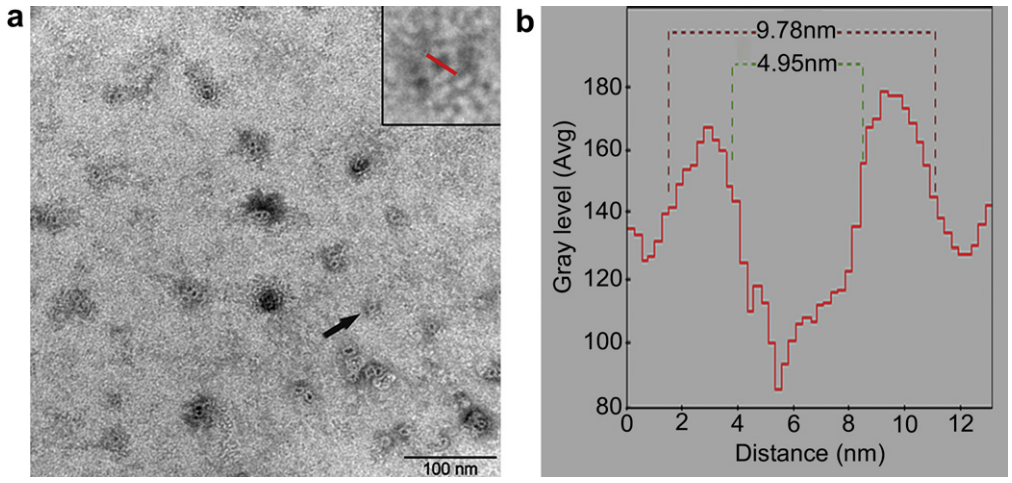

Fig. 2. TEM image revealed the size of well dispersed OPA-coated QDs. (a) TEM micrograph of OPA-coated QDs with 595 nm emission after negative staining by phosphotungstic acid. A further enlarged image is shown in a square inset for measurement of the QD size. Scale bar = 100 nm. (b) The size profile along the red line. (For interpretation of the references to colour in this figure legend, the reader is referred to the web version of this article.)

2.5. FISH

Maize metaphase chromosome spreads and interphase nuclei were prepared using the flame drying technique as described previously [27]. FISH was performed using the procedure according to a previous study [28]. The hybridization mixture contained 50% (v/v) deionized formamide, 2 × saline sodium citrate (SSC), 1 mg/ml of sheared salmon sperm DNA and 1–2 μg/ml probes. After overnight hybridization at 37 °C in a humid chamber, the slides were washed in 2 × SSC at RT for 10 min, 2 × SSC at 37 °C for 10 min, 2 × SSC at RT for 5 min, 1 × phosphate buffered saline (PBS) at RT for 5 min and then air dried. Slides were counterstained with 4′-6-diamidino-2-phenylindole (DAPI) and imaged on an Olympus BX-60 fluorescence microscopy. U-MWU filters (excitor 330–385 nm, dichroic mirror 400 nm, barrier 420 nm) and U-MWIG filters (excitor 510–550 nm, dichroic mirror 570 nm, barrier 590 nm) were employed in this study. Images were captured with a cooled CCD camera (1401E B0, Sensys, Photometrics, AZ, USA) by using Metamorph software (version 4.6r5, Universal Imaging, PA, USA).

3. Results and discussion

3.1. Characteristics of QDs and QD-oligonucleotide conjugates

To find out suitable QDs, which could endure the negative impact of PCR amplification, we tested different kinds of water-soluble QDs. QDs modified by polymers are brighter and more stable, thus making them suitable for PCR amplification [29]. In this study, QDs (the maximum emission wavelength, Em = 595 nm) coated with the amphiphilic octylamine-modified poly (acrylic acid) polymers were prepared (OPA-coated QDs, Fig. 1a). Steric hindrance is another key factor to affect QD-based PCR due to the comparatively large size of QDs. The TEM result shows that the core diameter of OPA-coated QDs was about 4.95 nm and the actual diameter including core and surface coating was about 9.78 nm, and displays well dispersed QDs without aggregation (Fig. 2a and b). The result demonstrated that the synthesized OPA-coated QDs had a relatively small size compared to the commonly used streptavidin-conjugated QDs (SA–QDs) (20–30 nm). Then the 5′ amine-modified oligonucleotide primers were covalently coupled to the surface of OPA-coated QDs as shown in Fig. 1b. The mean hydrodynamic diameter of QD-oligonucleotide conjugates was 17.26 ± 0.41 nm with a narrow size distribution that was larger than OPA-coated QDs (9.94 ± 0.07 nm) as determined by DLS measurement (Fig. 3), indicating that oligonucleotides have been attached to OPA-coated QDs.

In order to know if the synthesized QD-oligonucleotide conjugates could apply to further PCR amplification, we examined the effect of temperatures on the properties of OPA-coated QDs, because the main character of PCR is thermal cycling, including alternately heating and cooling. As shown in Fig. 4, the fluorescence intensity

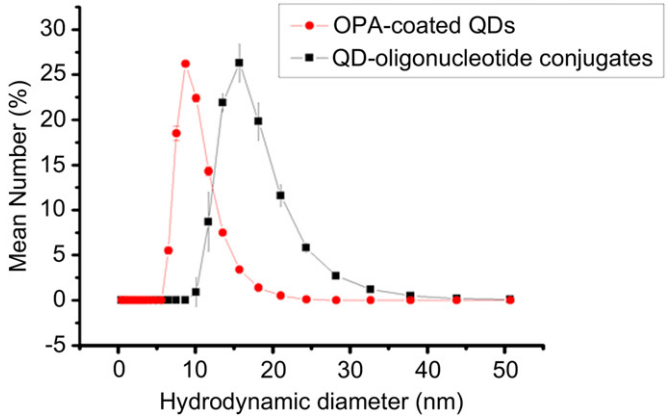

Fig. 3. Dynamic light scattering (DLS) measurements of the distribution of hydrodynamic diameter of OPA-coated QDs (red line) and QD-oligonucleotide conjugates (black line). Error bars represented standard deviations from multiple trials. (For interpretation of the references to colour in this figure legend, the reader is referred to the web version of this article.)

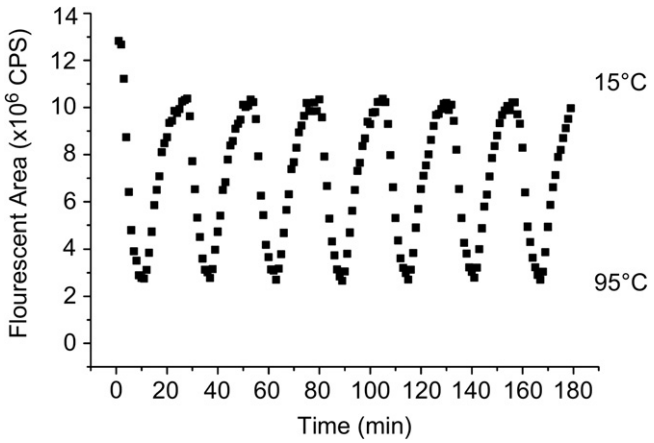

Fig. 4. The effect of the temperature on fluorescence intensity of OPA coated-QDs.

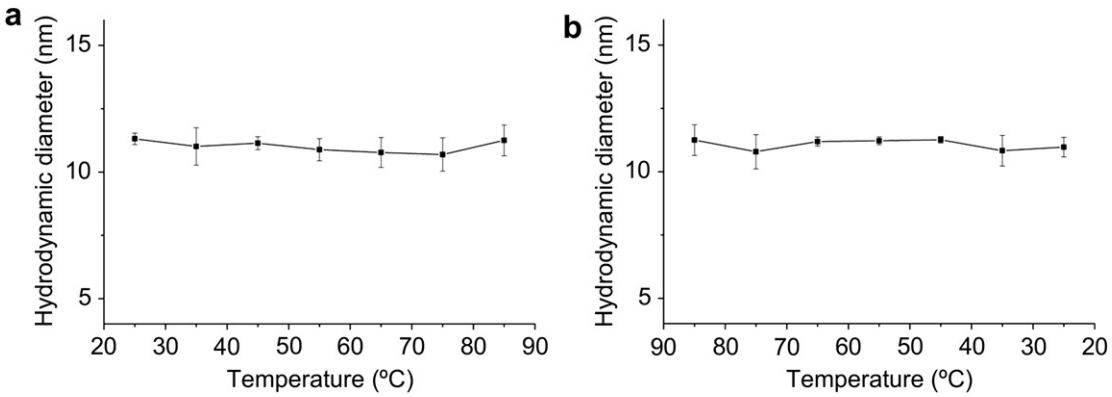

Fig. 5. The effect of the temperature on hydrodynamic diameter of OPA-coated QDs. (a) the temperature increasing period (from 25 °C to 85 °C). (b) the temperature declining period (from 85 °C to 25 °C). Error bars represent standard deviations from multiple trials.

declined with the increase in temperature (from 15 °C to 95 °C), but the effect was reversed when the temperature returned back (from 95 °C to 15 °C), except the first cycle. The fluorescence recovery efficiency of the first cycle hardly reached the original intensity because partial OPA-coated QDs were not perfectly assembled, and these unstable QDs were irreversibly quenched in the first cycle of heating-cooling. The fluorescence of the rest QDs was more stable in the following cycles. The OPA-coated QDs still possessed the original size under a representative heating–cooling cycle (from 25 °C to 85 °C, Fig. 5). Our results demonstrated that the synthesized OPA-coated QDs could endure thermal cycling and could be the most competitive candidate for PCR amplification.

3.2. Gel electrophoresis analysis of QD-based PCR products

Here, we report on the use of OPA-coated QDs as a supporting surface for PCR amplification of DNA to get substantial long DNA strands coupled with QDs under the above-mentioned optimizing conditions (Fig. 1c). After PCR reaction, gel electrophoresis experiment was carried out to investigate if QD-oligonucleotide conjugates were successfully extended. The band of QD-based PCR products (lane 2), QD-oligonucleotide conjugates (lane 3) and QDs (lane 4) could be seen under UV excitation due to QD luminescence although the gel was not stained with ethidium bromide (EB), while the band of normal PCR products (lane 1) could not be seen in the gel (Fig. 6a). It was confirmed that the QD-labeled long DNA strands were successfully obtained after QD-based PCR reaction by sequencing of DNA extracted from the band in lane 2 (Fig. 6a). The DNA sequence is the same as the reported result [30]. The electrophoretic mobility of QD-labeled long DNA strands (lane 2, Fig. 6) is slower than QD-oligonucleotide conjugates (lane 3, Fig. 6) because of the increase of overall size after PCR synthesis. And the mobility of QD-oligonucleotide conjugates (lane 3, Fig. 6) is also slower than OPA-coated QDs (lane 4, Fig. 6) due to the size increase of QD-oligonucleotide conjugates. The remaining free DNA oligonucleotides were completely removed from QD-oligonucleotide conjugates monitored with EB staining (lane 3, Fig. 6b). Another lower band appeared in lane 2 (Fig. 6b) after EB staining whose electrophoretic mobility and DNA sequence were same as those of normal PCR products (lane 1, Fig. 6b). Appearance of the lower band in QD-based PCR products suggested that the partial oligonucleotides or long DNA strands might detach from the QD surfaces during PCR processes because of the terrible conditions in PCR. Although great efforts were made to avoid aggregation of QDs in the terrible conditions, this phenomenon still happened to partial QDs, which stay inside the loading lane (lane 2, Fig. 6a).

In the QD-based PCR process, once one of the oligonucleotides on the QD surface was extended by DNA polymerase, the synthesized

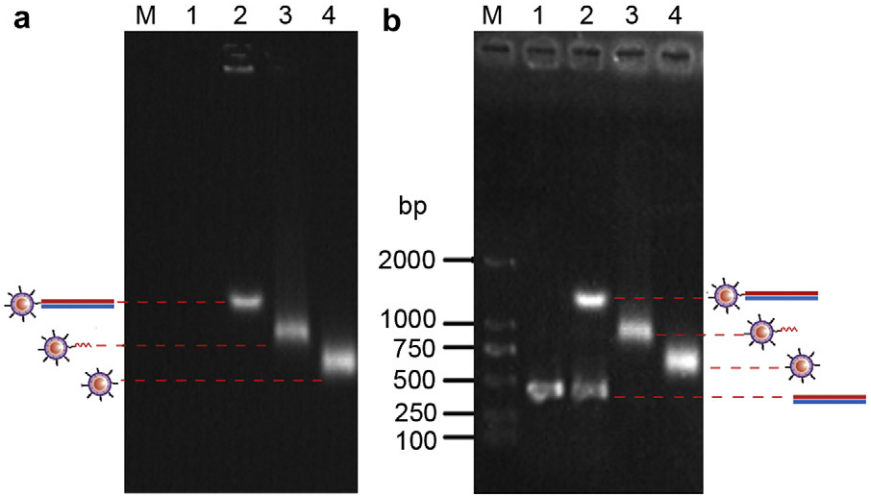

Fig. 6. Gel electrophoresis for verification of QDs conjugated with DNA. (a) Before stained with EB. (b) After stained with EB. Lane M: DNA marker (DL 2000); lane 1: normal PCR products; lane 2: QD-based PCR products; lane 3: QD-oligonucleotide conjugates; lane 4: OPA-coated QDs.

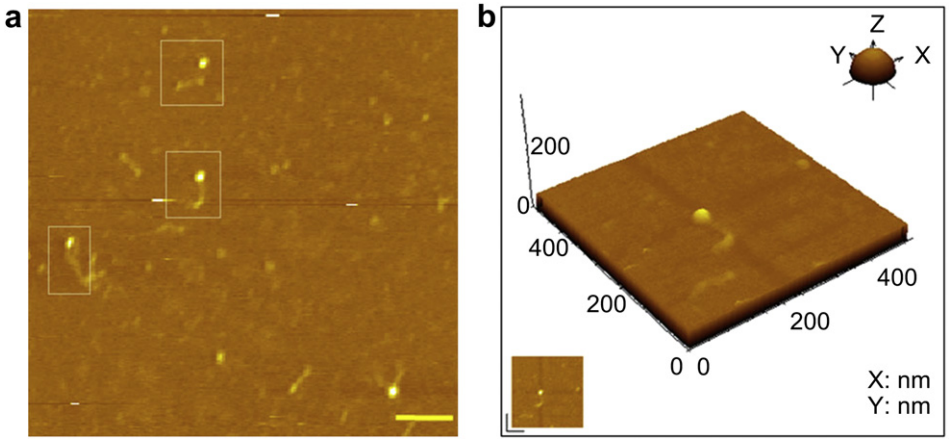

Fig. 7. The AFM image of the QD-labeled long DNA strand purified by DNA Gel Extraction Kit. (a) A 2-D AFM image of the QD-labeled long DNA strand revealing one long synthesized DNA strand linked to a QD, which is marked by a white rectangle (large scale, 1500 nm × 1500 nm). Scale bar = 200 nm. (b) A 3-D AFM image of the QD-labeled a single long DNA strand (small scale, 500 nm × 500 nm).

480-bp-long DNA might greatly increase the local steric hindrance on the QD surface that would hinder both annealing step and extension step, so the following extension of the rest oligonucleotides on the QD surface was hardly performed. Therefore, we speculated that most of the products should be QD-labeled single long DNA strands. As expected, it was found that the band containing QD-labeled long DNA strands (lane 2) was narrower than the band of QD-oligonucleotide conjugates (lane 3) and QDs (lane 4) in Fig. 6a and b, which indicated that the population of QD-labeled long DNA strands were more homogeneous in charge and particle size distribution. Our results implied that the obtained products were QD-labeled single long DNA strands.

3.3. AFM visualization of QD-labeled long DNAs

To further confirm that only a single long DNA was bound to a single QD, the QD-labeled long DNA strands (lane 2, Fig. 6a) were excised from the gel, purified by the AxyPrep DNA Gel Extraction Kit (Axygen Biosciences, CA, USA), and imaged by AFM. From a large scale AFM image (1500 nm × 1500 nm, Fig. 7a), several single QD-labeled single long DNA strands were observed. The detail was further observed in a small scale (500 nm × 500 nm, Fig. 7b). In the small scale image, the height of the DNA strand was ca. 1 nm and the length was ca. 160 nm, which corresponded to a 480 bp DNA strand. Therefore, in this study, by combining QD-based PCR and electrophoretic separation, we successfully obtained one-to-one QD-labeled single long DNA conjugates.

Monofunctional nanoparticle was viewed as one of most important research goals in nanobiotechnology [7,8,31]. Successful amplification of a single long DNA conjugated with a single QD is critical to sequence-specific DNA detection.

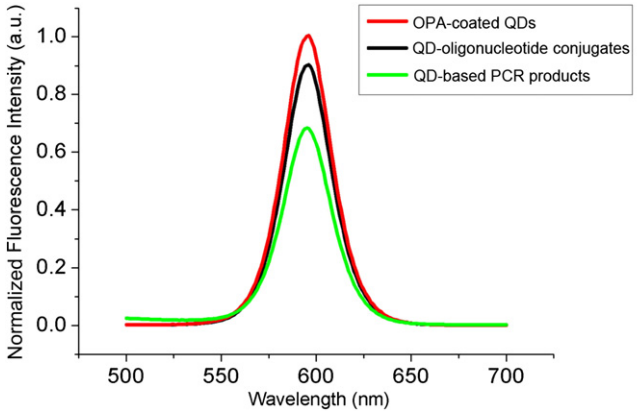

Fig. 8. Fluorescence spectra of OPA coated-QDs (red line), QD-oligonucleotide conjugates (black line) and QD-based PCR products (green line) under 595 nm emission. (For interpretation of the references to colour in this figure legend, the reader is referred to the web version of this article.)

3.4. Fluorescence property

Fluorescence spectrum measurement revealed that the emission peak of QD-oligonucleotide conjugates and QD-based PCR products did not shift, which was the same as that of QDs, and the fluorescence intensity of QD-oligonucleotide conjugates and QD-based PCR products just slightly reduced (Fig. 8). Therefore the fluorescence properties of QDs were well conserved during couple reaction and PCR reaction, indicating that QD-labeled single long DNA strands could be used as fluorescence probes.

3.5. Bioactivity of QD-Labeled single long DNAs

FISH experiments were performed to assess the biological activity of the obtained one-to-one QD-labeled single long DNA probes. The full length of a single copy gene (*fatty aldehyde dehydrogenase 1*, *rf2e1*, 4793 bp) has been mapped on maize chromosomes by a routine FISH [30]. Fig. 9a and c showed the FISH signals on prometaphase chromosomes and in nuclei. The double red dots were present on two sister chromatids and located in the middle of the long arms of metaphase chromosomes (Fig. 9b), which was consistent with the reported locations [30]. The QD-labeled long DNA probes were shown to bind to complementary target sequences on chromosomes immobilized on a slide surface, but not to noncomplementary chromosomal regions. The control of employing solely OPA-coated QDs without the attachment of oligonucleotides as probes showed no specific hybridization signals present on chromosomes and in a nucleus (Fig. 9d and e). These results demonstrated biological activity of the one-to-one QD-labeled long DNA probes and specificity of the hybridization signals.

Although a DNA fragment of a single copy gene (480 bp) was mapped on chromosomes in this study, the detection of a small and single copy of DNA on metaphase chromosomes, especially for large complex plant genomes, still represents an experimental challenge

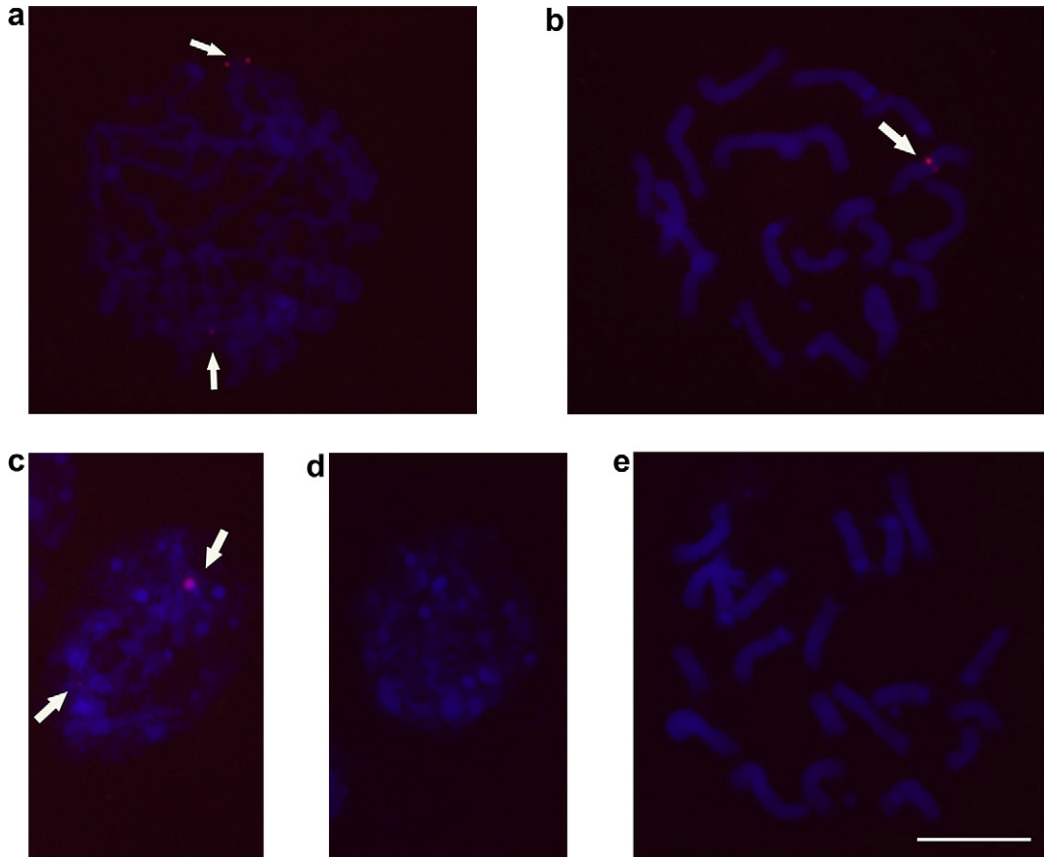

Fig. 9. Specificity of the one-to-one QD-labeled single long DNA probes to detect *rf2e1* gene on maize chromosomes and in nuclei. (a) Signals on prometaphase chromosomes. (b) Signals on metaphase chromosomes. (c) Signals in a nucleus. (d) A control experiment with OPA-coated QDs in a nucleus. (e) A control experiment with OPA-coated QDs on chromosomes. Signals are indicated by white arrows. Scale bar = 10 μm.

for using QD-based detection. The current preliminary result provides useful experimental data regarding use of QDs for fluorescence detection of DNA sequences and thus paves the way towards small single copy of DNA fragment detection and the use of QD-DNA conjugates as fluorescence probes for multicolor FISH of different genes on chromosomes. In addition to mapping DNA on chromosomes, it should also be possible for QD-labeled single long DNA strands by PCR to probe complementary target sequences in DNA microarrays, fixed sectioned tissues, or nitrocellulose blots.

4. Conclusion

We have reported a modified PCR strategy to construct one-to-one QD-labeled single long DNA probes, which will play an important role in the detection of small single-copy DNA fragments, quantitative analysis and single molecule imaging, as well as possible fabrication of more complex nanostructure. The ability of PCR amplification of any different genes or DNA sequences with QD-oligonucleotides as primers would allow multicolor labeling of cells and chromosomes in a single mapping procedure and provide expansive labeling and imaging applications in biology. The method established in this study is expected to be generally applicable for all enzymatic reactions based on QDs and to spur on more applications of nanoparticles in medical diagnosis and basic biological research as well as material fabrication.

Acknowledgments

This work was supported by the NSFC (Nos. 30870261, 20921062, 20875071), the National genetically modified organism breeding major project (No. 200908010-008B), the Research Fund for the Doctoral Program of Higher Education (NO. 20090141110031) and the National Key Scientific Program (973)-Nanoscience and Nanotechnology (No. 2011CB933600).

References

[1] Michalet X, Pinaud FF, Bentolila LA, Tsay JM, Doose S, Li JJ, et al. Quantum dots for live cells, in vivo imaging, and diagnostics. Science 2005;307:538–44.
[2] Medintz IL, Uyeda HT, Goldman ER, Mattoussi H. Quantum dot bioconjugates for imaging, labelling and sensing. Nat Mater 2005;4:435–46.
[3] Smith AM, Nie SM. Next-generation quantum dots. Nat Biotechnol 2009;27:732–3.
[4] Jamieson T, Bakhshi R, Petrova D, Pocock R, Imani M, Seifalian AM. Biological applications of quantum dots. Biomaterials 2007;28:4717–32.
[5] Ma L, He S, Huang J, Cao L, Yang F, Li L. Maximizing specificity and yield of PCR by the quantum dot itself rather than property of the quantum dot surface. Biochimie 2009;91:969–73.
[6] Aldaye FA, Palmer AL, Sleiman HF. Assembling materials with DNA as the guide. Science 2008;321:1795–9.
[7] Carstairs HMJ, Lymperopoulos K, Kapanidis AN, Bath J, Turberfield AJ. DNA monofunctionalization of quantum dots. Chembiochem 2009;10:1781–3.
[8] Boeneman K, Deschamps JR, Buckhout-White S, Prasuhn DE, Blanco-Canosa JB, Dawson PE, et al. Quantum dot DNA bioconjugates: attachment chemistry strongly influences the resulting composite architecture. ACS Nano 2010;4:7253–66.
[9] Zanchet D, Micheel CM, Parak WJ, Gerion D, Alivisatos AP. Electrophoretic isolation of discrete Au nanocrystal/DNA conjugates. Nano Lett 2001;1:32–5.
[10] Fu A, Micheel CM, Cha J, Chang H, Yang H, Alivisatos AP. Discrete nanostructures of quantum dots/Au with DNA. J Am Chem Soc 2004;126:10832–3.
[11] Arnheim N, Erlich H. Polymerase chain reaction strategy. Annu Rev Biochem 1992;61:131–56.
[12] Adessi C, Matton G, Ayala G, Turcatti G, Mermod JJ, Mayer P, et al. Solid phase DNA amplification: characterisation of primer attachment and amplification mechanisms. Nucleic Acids Res 2000;28:e87.
[13] Chen W, Bian A, Agarwal A, Liu L, Shen H, Wang L, et al. Nanoparticle superstructures made by polymerase chain reaction: collective interactions of

nanoparticles and a new principle for chiral materials. Nano Lett 2009;9: 2153–9.
[14] Nicewarner Pena SR, Raina S, Goodrich GP, Fedoroff NV, Keating CD. Hybridization and enzymatic extension of au nanoparticle-bound oligonucleotides. J Am Chem Soc 2002;124:7314–23.
[15] Qin WJ, Yung LY. Nanoparticle-DNA conjugates bearing a specific number of short DNA strands by enzymatic manipulation of nanoparticle-bound DNA. Langmuir 2005;21:11330–4.
[16] Patolsky F, Gill R, Weizmann Y, Mokari T, Banin U, Willner I. Lighting-up the dynamics of telomerization and DNA replication by CdSe-ZnS quantum dots. J Am Chem Soc 2003;125:13918–9.
[17] Xiao Y, Barker PE. Semiconductor nanocrystal probes for human metaphase chromosomes. Nucleic Acids Res 2004;32:e28.
[18] Pinaud F, Michalet X, Bentolila LA, Tsay JM, Doose S, Li JJ, et al. Advances in fluorescence imaging with quantum dot bio-probes. Biomaterials 2006;27: 1679–87.
[19] Chen C, Peng J, Xia HS, Yang GF, Wu QS, Chen LD, et al. Quantum dots-based immunofluorescence technology for the quantitative determination of HER2 expression in breast cancer. Biomaterials 2009;30:2912–8.
[20] Wang Z, Lu M, Wang X, Yin R, Song Y, Le XC, et al. Quantum dots enhanced ultrasensitive detection of DNA adducts. Anal Chem 2009;81:10285–9.
[21] Jiang J, Gill BS. Current status and the future of fluorescence in situ hybridization (FISH) in plant genome research. Genome 2006;49:1057–68.
[22] Xie HY, Liang JG, Liu Y, Zhang ZL, Pang DW, He ZK, et al. Preparation and characterization of overcoated II-VI quantum dots. J Nanosci Nanotechnol 2005;5:880–6.
[23] Zhou M, Nakatani E, Gronenberg LS, Tokimoto T, Wirth MJ, Hruby VJ, et al. Peptide-labeled quantum dots for imaging GPCRs in whole cells and as single molecules. Bioconjug Chem 2007;18:323–32.
[24] Choi Y, Kim HP, Hong SM, Ryu JY, Han SJ, Song R. In situ visualization of gene expression using polymer-coated quantum-dot-DNA conjugates. Small 2009; 5:2085–91.
[25] Ma L, Wu SM, Huang J, Ding Y, Pang DW, Li L. Fluorescence in situ hybridization (FISH) on maize metaphase chromosomes with quantum dot-labeled DNA conjugates. Chromosoma 2008;117:181–7.
[26] Porebski S, Bailey LG, Baum BR. Modification of a CTAB DNA extraction protocol for plants containing high polysaccharide and polyphenol components. Plant Mol Biol Rep 1997;15:8–15.
[27] He S, Huang M, Huang J, Li J, Hu Y, Zhang L, et al. Dynamics of the Evolution of the Genus of *Agrostis* revealed by GISH/FISH. Crop Sci 2009;49:2285–90.
[28] Huang J, Ma L, Yang F, Fei SZ, Li L. 45S rDNA Regions are chromosome Fragile Sites Expressed as Gaps in vitro on metaphase chromosomes of Root-Tip Meristematic cells in *Lolium* spp. PLoS One 2008;3:e2167.
[29] Pellegrino T, Manna L, Kudera S, Liedl T, Koktysh D, Rogach AL, et al. Hydrophobic nanocrystals coated with an amphiphilic polymer shell: a general Route to water soluble nanocrystals. Nano Lett 2004;4:703–7.
[30] Lamb JC, Danilova T, Bauer MJ, Meyer JM, Holland JJ, Jensen MD, et al. Single-gene detection and karyotyping using small-target fluorescence in situ hybridization on maize somatic chromosomes. Genetics 2007;175:1047–58.
[31] Howarth M, Liu W, Puthenveetil S, Zheng Y, Marshall LF, Schmidt MM, et al. Monovalent, reduced-size quantum dots for imaging receptors on living cells. Nat Methods 2008;5:397–9.